# A MICRODISCHARGE-BASED RADIATION DETECTOR UTILIZING STACKED ELECTRODE ARRAYS IN A TO-5 PACKAGE

*Christine K. Eun*[1] *and Yogesh B. Gianchandani*
Center for Wireless Integrated Microsystems (WIMS)
Department of Electrical Engineering and Computer Science, University of Michigan
[1]1301 Beal Avenue, Ann Arbor, Michigan, USA, e-mail: eunc@umich.edu

## ABSTRACT

This paper describes miniature discharge-based beta/gamma radiation detectors that use arrayed electrode structures to demonstrate a scalable path for increasing detection efficiency. The discharges are also used for wireless signaling. The device uses an in-package assembly scheme of stainless steel electrodes and a glass spacer structure within a TO-5 package. It is manufactured by leveraging commercial micromachining technologies e.g., photochemical etching of the electrodes and ultrasonic machining of the spacer structure. The detector diameter and height are 9 mm and 9.6 mm, respectively, and it weighs 1.01 g. The device performance has been characterized using a P-10 fill-gas near 710 Torr, with a 99 μCi $^{137}$Cs source (which is a beta and gamma emitter). The normalized gamma sensitivity is estimated to be 0.023 cps/mR/hr/mm$^3$ as measured with the biasing arrangement described in the paper. Portable powering modules developed for these detectors are also presented. Rapid wireless transmissions with durations on the order of tens of ns have been measured.

## INTRODUCTION

There is increasing interest in microsystems that can provide real-time, first alert information on the presence of dangerous radioisotopes. Miniaturized radiation detectors can serve applications ranging from monitoring radiation safety levels of nuclear power plants to guarding against illicit trafficking of radioactive chemicals and port screening for homeland security. These can lead to ultra-portable and reconfigurable sensor network systems [1-2], lower power requirements, and permit the use of lithographic manufacturing to drive down sensor cost. In addition, leveraging existing commercial, hermetic packages can enable cost-effective, fast prototyping and large-scale manufacturing. For example, TO-5 headers have been used to package miniaturized gas-based radiation detectors [3-4].

Oftentimes, when a radioisotope undergoes decay, a combination of radiation types is emitted. For example, when $^{137}$Cs decays, it emits beta particles (with an endpoint energy of 0.514 MeV) 94.4% of the time and gamma-rays (with an energy of 0.662 MeV) 85.1% of the time [5]. This type of radiation source may be detected by either a beta detector or a gamma detector. Of course, a detector that is responsive to both beta and gamma radiation is likely to measure a higher signal from such a source.

Gas-based detectors (e.g., Geiger counters) are often favored for environmental surveillance efforts (e.g., in looking for radiation leaks and inadvertent contamination) [6]. These are relatively simple and robust, and can operate over a large temperature range, and measure a wide range of radiation species and energies. The basic structure of a detector includes two biased electrodes (anode and cathode) enclosed within a gas-filled chamber. Beta-particles directly interact with the gas, causing avalanche discharges, with current pulses that register as "counts." Under appropriate conditions, electrical discharges such as these can emit broadband radio frequency radiation in the manner of Marconi transmitters [7]. It has been shown that microdischarges can be used for wireless signaling [8].

Gas-based detection of gamma radiation relies on converting the photons into photoelectrons; these ejected photoelectrons then ionize the fill-gas and trigger micro-discharges [9]. The conversion is typically facilitated by using high-density metals for the electrodes and for the walls encapsulating the fill-gas. The use of high-pressure, large atomic number fill-gases [10] can also increase the interaction probability. Gamma radiation interacts with materials in primarily three collision processes, i.e., the photoelectric effect, Compton scattering, and pair production. The energy of the incoming photon determines the collision process.

One inherent limitation of gas-based detectors is the low-density nature of the gaseous detection medium, which results in low detection efficiencies (1-2% [6]), in particular with gamma and neutron radiation. Utilizing stacks of electrodes within a detector structure can potentially increase detection efficiencies for a given form factor.

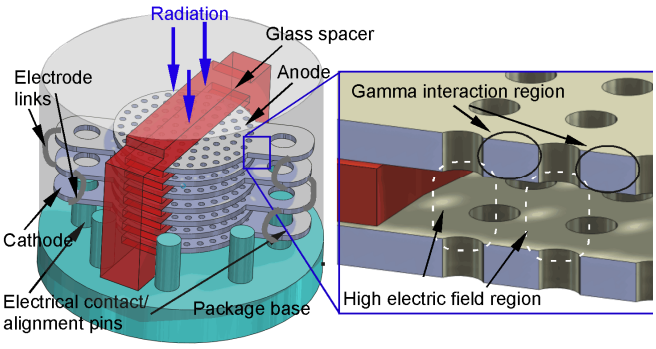


*Figure 1: Device concept. The detector comprises an arrayed arrangement of multi-element stainless steel electrodes (i.e., anode and cathode) and a glass insulator, assembled within a commercial TO-5 package base. Gamma radiation interacts with the metal layers, which releases photoelectrons into the biased gap. These charged particles trigger avalanche within the biased gap, leading to wireless signaling.*

Past work on stacking detector structures in order to achieve improved performance includes a variation on the GEM detector [11]. GEM structures involve thin Kapton

film substrates with double-sided metal laminates (1 to 5 μm-thick) and chemically-etched perforations. An applied voltage generates concentrated electric fields (50-70 kV/cm) at the edges of these etched features, which accelerates the ionized particles through the openings. The triple GEM detector utilizes the parallel stacking of three GEM structures in order to increase the amplification of the carriers (or gain) at lower bias conditions (as compared to a single GEM). GEM structures are typically used for particle tracking applications, where portability and gas packaging are not limiting factors. These stacked structures require several bias voltages (i.e., for the drift and readout plate and each GEM layer). In addition, these structures do not focus on achieving high detection efficiency, but rather high position resolution of the particle trajectory.

This paper demonstrates a scalable path for increasing detection efficiency for small form factors by utilizing an arrayed electrode structure. This particular approach focuses on maximizing the overall effective sensitive volume by increasing the number of sensing gaps, increasing the amount of high-Z materials (e.g., 150-μm-thick metal foils) for increased gamma interaction, and utilizing the entire volume of a given package (e.g., for this effort, a TO-5 header). In addition, a unique construction method facilitates assembly and operation with a single bias voltage, while the thick micromachined metal foils provide increased lifetime.

## DEVICE CONCEPTS

The detector structure includes two sets of perforated, stainless steel #304 electrode arrays (the anode has 4 elements and the cathode has 3 elements). The elements in each set are connected by v-shaped links. Each set is designed to be plastically deformed into a stack of parallel elements. These elements are inserted into an insulating glass structure with micromachined shelves, which maintains a 200 μm-wide anode-cathode gap-spacing (Fig. 1). An applied bias generates high-field regions near the perforations. Beta radiation directly interacts with the fill-gas, whereas gamma radiation mostly interacts with the steel electrodes to generate photoelectrons. Beta radiation or photoelectrons initiate current-driven avalanche pulses between the biased electrodes, which transmit wideband wireless signals.

### Electric Field Modeling

Finite element analysis (FEA) using COMSOL 3.5a modeled the electric field profile of the arrayed electrode configuration (Fig. 2a). The simulations show that with a 200-μm gap-spacing and a bias level of 600 V, a maximum electric field of approximately 4-5 MV/m is generated near the perforation corners. The wet etching process that forms the perforations results in a slight sloped profile and a peak-like feature at the center of the perforation. There is a 50 μm difference in hole diameter from the top of the perforation to its center. These peak features result in increased field strengths (approximately 75% higher for a given bias voltage) within the perforation compared to straight side-walls. An SEM image illustrates the peak features and asperities (Fig. 2b).

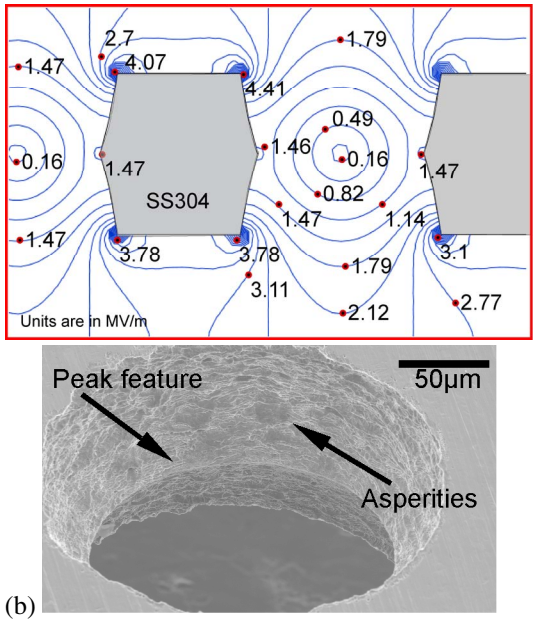


*Figure 2: Electric field modeling with $V_{applied}$ = 600V (a) A magnified view of the field profile near the perforation feature. Units are in MV/m. (b) SEM images of the perforations show a top diameter of 225 μm and center diameter of 175 μm.*

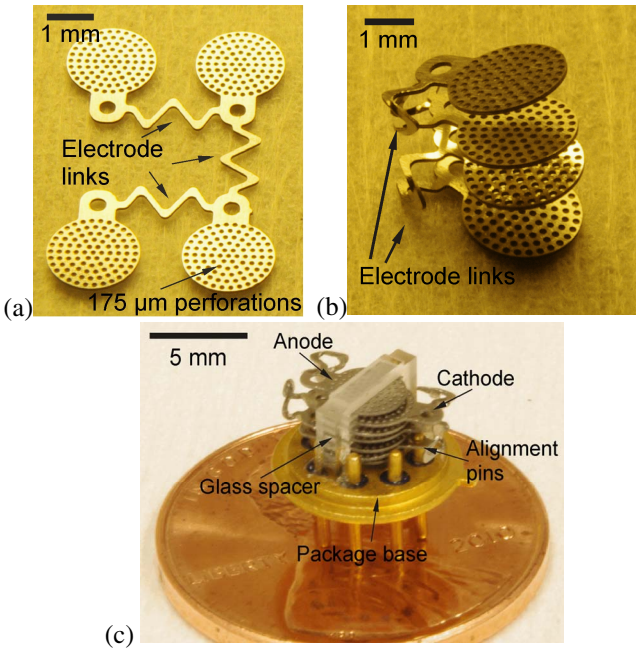


*Figure 3: Device assembly. (a) Beginning with a planar arrangement of linked elements, (b) each element is folded at the link to create an accordion pattern. (c) The folded anode and cathode are placed within the glass spacer, separated by machined shelves and into the package base using the alignment pins.*

## FABRICATION AND ASSEMBLY

The detector elements are manufactured by commercial processes. The electrodes (i.e., 150 μm-thick stainless-steel #304) are lithographically-patterned with resist and photochemically-etched using a hot etchant spray. In this design, 175 μm-diameter circular perforations are formed, with 300 μm center-to-center spacing. The glass spacer is formed by ultrasonic machining a 1.14 mm-thick borosilicate-glass substrate. The machined shelves are 200 μm-thick and separated by 200 μm-gaps.

Each electrode array begins planar (Fig. 3a), and is plastically-bent at the links to form parallel elements (Fig. 3b). To facilitate assembly, each steel element is designed with openings to align with the package pins. The electrode array is inserted into the glass spacer, which fits between adjacent pins (Fig. 3c). The package is an 8-pin TO-5 header with a 9 mm diameter and 9.6 mm height. The overall device weighs 1.01 g. Electrical feed-throughs are available as pins through the package base.

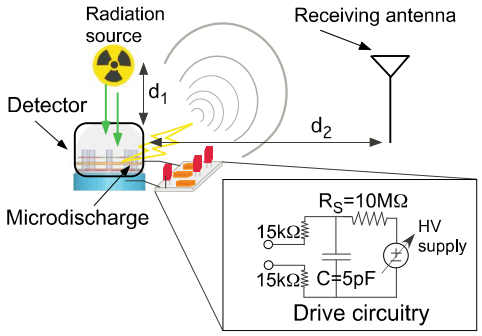


*Figure 4: The test setup with the device and bias circuitry (positioned at distance, $d_1$, from the radiation source). Current pulses were measured at the cathode with an inductive current probe attached to an oscilloscope. Wireless measurements were performed with a receiving antenna attached to an oscilloscope at distance, $d_2$, from the detector.*

## EXPERIMENTAL RESULTS

The detector structure was operated with a P-10 fill-gas (i.e., 90% Ar and 10% $CH_4$) near 710 Torr with a small 99 μCi radiation source of $^{137}Cs$, which emits both beta and gamma radiation. Wireline measurements of the count rate were obtained with a high-frequency inductive current probe attached to an oscilloscope. Wireless measurements were received using an 800 MHz whip antenna connected to an oscilloscope. The detector was powered by a custom designed PCB, which housed the detector bias circuit and the HV converter circuitry.

### Wireline Measurements

The current pulses had 20–50 ns duration and 100 mA peak amplitudes (Fig. 5a). The majority of the oscillations are attributed to artifacts associated with the inductive current probe. Figure 6 illustrates the impact of applied bias on typical counting rates. The rates increased 6X for a 10V increase in applied bias. The background counts produced a slower rate of increase (2X). At 450 V bias, typical count rates were near 300 cpm at a source-detector distance of 4 cm. Measured background rates (i.e., in the absence of a radiation source) ranged from 0-50 cpm.

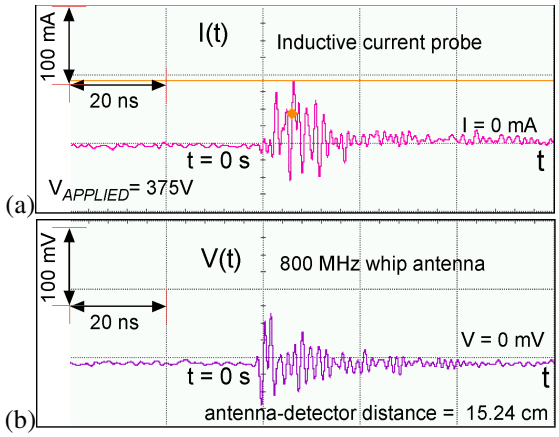


*Figure 5: (a) Current pulse measurement (of a "count") showed approx. 100 mA peaks and 20–50 ns duration. (b) The transmitted wireless signal was received using an 800 MHz whip antenna attached to an oscilloscope. The antenna-detector distance was 15.24 cm. The time domain behavior of the RF signal followed closely with the current pulses. A radiation source of 99 μCi $^{137}Cs$ was used.*

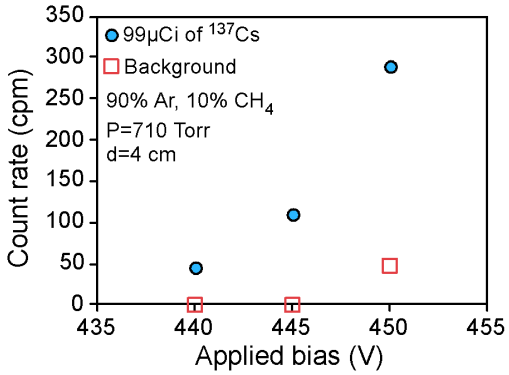


*Figure 6: Typical count rates as a function of applied bias in a 90% Ar and 10% $CH_4$ fill-gas near 710 Torr. Background rates increase at a slower rate. A 99 μCi $^{137}Cs$ source was positioned 4 cm from the detector.*

### Wireless Measurements

The transmitted wireless spectra (Fig. 5b) received at an antenna-detector distance of 15.24 cm, followed closely with the current pulse measurement (Fig. 5a). The transient behavior of the wireless signal with durations on the order of tens of ns was observed.

### PCB powering module

In order to have a standalone micro-detector system, the powering module and readout scheme that interfaces with the micro-detector must be efficient, compact, light-weight, and battery-operated. The required components for the powering module include a battery source, an adjustable voltage regulator, a high-voltage converter, the detector bias circuitry, and a readout scheme (Fig. 7a). A PCB power module has been designed and populated (Fig. 7b).

The readout scheme should be simple and reliable. An optical readout offers instantaneous signaling and requires no additional wiring or measurement equipment. Positioning the LED in the current path of the detector can assure that each triggered event will generate an optical signal. However, this scheme would require the current output from the detector to be high enough to turn on the LED. The optical LED can be interchanged with an IR LED along with an IR receiver positioned in the proximity (approx. 10 m) of the detector board.

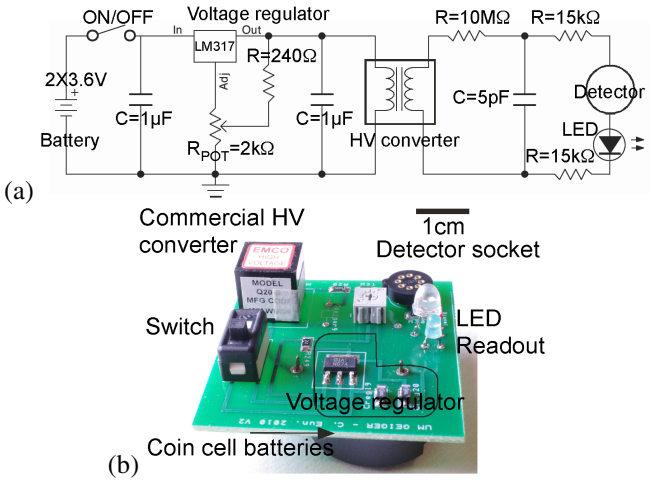


*Figure 7: (a) A circuit schematic and (b) populated PCB of a HV powering module for the detector. It included coin cell batteries, a voltage regulator circuit, a commercial high voltage converter, the detector bias circuit, and the LED readout. The total PCB weighs 26.5 g (with batteries).*

## CONCLUSIONS

An arrayed electrode structure was used to demonstrate a scalable path for increasing detection efficiency for miniature radiation detectors based on gas-discharges. The average measured count rate was >5 cps for a source-detector distance of 4 cm with a 99 μCi $^{137}$Cs source. The performance of the multi-stacked arrayed detector compared to a commercial, off-the-shelf (COTS) GM tube is summarized in Table 1. The arrayed detector displayed a gamma sensitivity that was 2X better than the COTS unit when normalized to detector sensitive volume. The detector sensitive volume is the total volume encapsulated between the anode and cathode. (The arrayed detector volume was only 3% the volume of the COTS device.) The background rates from the micro-detectors were higher than the COTS unit, which was expected since the arrayed detectors were unshielded.

## ACKNOWLEDGEMENTS

This work was supported by the Dept. of the Army, Micro Autonomous Systems and Technology (MAST) Collaborative Technology Alliance, Contract No. W911NF-08-2-0004.

*Table 1: A comparison of the arrayed detector with a commercial of the shelf (COTS) GM tube.*

| | LND 726 (COTS GM tube) | Arrayed Detector |
|---|---|---|
| Gas filling | 95%Ne+1%$Cl_2$ | 90%Ar+10%$CH_4$ |
| Cathode material | 446 Stainless Steel | 304 Stainless Steel |
| Max. length (mm) | 49.8 | 9.6 |
| [1]Eff. length (mm) | 10.2 | 0.90 |
| Max. diam. (mm) | 8.7 | 9 |
| [1]Eff. diam. (mm) | 6.4 | 1.94 |
| Volume ($mm^3$) | 328 | 10.62 |
| Operating voltage range (volts) | 660 - 800 | 440 - 575 |
| [2]Normalized gamma sensitivity (cps/mR/hr/$mm^3$) | 0.010 ($^{60}$Co) | 0.023[3] ($^{137}$Cs) |
| Background rates | 10 cpm (shielded w/ 50 mm Pb & 3 mm Al) | 50 cpm (unshielded) |
| Weight (grams) | 10 | 1.01 |

[1] *Effective length/diameter refers* to sensitive region of detector
[2] Sensitive volume refers to volume between anode/cathode.
[3] Measured with an exposure rate of 20 mR/hr calibrated with 99μCi of $^{137}$Cs at d = 4cm.

## REFERENCES

[1] R.J. Nemzek, J.S. Dreicer, D.C. Torney, and T.T. Warnock, "Distributed sensor networks for detection of mobile radioactive sources," *IEEE Trans. on Nuclear Science*, vol. 51, no. 4, Aug. 2004, pp. 1693-1700.

[2] R. Kyker, N. Berry, D. Stark, N. Nachtigal, and C. Kershaw, "Hybrid Emergency Radiation Detection (HERD), a wireless sensor network application for consequence management of a radiological release," *Proceedings of SPIE*, vol. 5440, pp. 293-304.

[3] C.K. Eun, R. Gharpurey, and Y.B. Gianchandani, "A wireless-enabled radiation detector using micromachined steel and glass elements in a TO-5 package," *A Solid-State Sensors, Actuators and Microsystems Workshop 2010*, Hilton Head Island, SC, pp. 380-382.

[4] C.K. Eun and Y.B. Gianchandani, "A microfabricated steel and glass radiation detector with inherent wireless signaling," *Journal of Micromechanics and Microengineering*, Nov. 2010, *in press.*

[5] R.B. Firestone and L.P. Ekstrom, "LBNL Isotopes Project," LUNDS Universitet, Ver. 2.1, Feb. 1999.: http://ie.lbl.gov/toi/index.asp

[6] G.F. Knoll, *Radiation Detection & Measurement*, Wiley, 2000

[7] J.E. Brittain, "Electrical engineering Hall of Fame: Guglielmo Marconi," *Proc. of the IEEE*, vol. 92, no. 9, pp. 1501-4, Aug 2004.

[8] C.K. Eun, R. Gharpurey, and Y.B. Gianchandani, "Wireless signaling of beta detection using microdischarges," *JMEMS*, vol. 19, no. 4, pp. 785-793, Aug. 2010.

[9] B. Shafrir and A. Seidman, "High efficiency gamma-ray metal converters," *Nuc. Instruments & Methods*, vol. 129, pp. 177-186, 1975.

[10] S.D. Kiff, Z. He, and G.C. Tepper, "A new coplanar-grid high-pressure xenon gamma-ray spectrometer," *IEEE Trans. on Nuclear Science,* vol. 52, no. 6, pp. 2932-2939, Dec. 2005.

[11] F. Sauli, "Gas detectors: achievements and trends," *Nuclear Instruments and Methods in Physics Research A*, vol. 461, pp. 47-54, 2001.